Composite Part B, 46:211–220, 2013.

Determination of Material Parameters for Abaqus Progressive Damage Analysis of E-Glass Epoxy Laminates

E. J. Barbero[1], F. A. Cosso [2], R. Roman[2], T. L. Weadon[2]
Mechanical and Aerospace Engineering, West Virginia University,
Morgantown, WV 26506-6106, USA

abstract

A methodology for determination of material parameters for the progressive damage analysis (PDA) model implemented in Abaqus is presented. The methodology is based on fitting PDA model results to available experimental data. The applicability of the PDA model is studied by comparison to a broad set of experimental data for E-Glass Epoxy laminates, as well as contrasting PDA with ply discount results.Also, sensitivity of the Abaqus PDA model to h- and p-refinement is studied.

keyword

A. Polymer-matrix composites (PMCs); B. Transverse cracking; C. Damage mechanics; C. Finite element analysis (FEA); Parameter Identification.

1 Introduction

Prediction of damage initiation and accumulation in polymer matrix, laminated composites is of great interest for the design, production, certification, and monitoring of an increasingly large variety of structures. It is also a complex and difficult topic. Only matrix cracking due to transverse tensile and shear deformations is considered in this manuscript. Matrix cracking is normally the first mode of damage. If left unmitigated, it often leads to other modes such as delamination and, due to load redistribution, may even lead to fiber failure of adjacent laminas.

The earliest, simplest and least accurate modeling technique to address matrix damage is perhaps the ply discount method [1, Section 7.3.1]. Ply discount is used here as a baseline for contrasting predictions obtained with the progressive damage analysis (PDA) method implemented in Abaqus™[3] [**?**]. Although many other models exist [2–12], etc., and several plugins are available [13, 14], this manuscript focuses on the PDA model available in Abaqus. This is because of the broad availability of Abaqus, while plugins are not free, and the remaining models available in the literature are for the most part not readily available to be used in conjunction with commercial FEA environments.

Therefore, the objective of this manuscript is to propose a methodology to determine values for the material parameters required by the Abaqus PDA model. In this work, the values for the parameters are found using available experimental data and a rational procedure. Once values are found, the PDA model is

[1]Corresponding author. The final publication is available at http://dx.doi.org/10.1016/j.compositesb.2012.09.069
[2]Graduate Research Assistant.
[3]Abaqus and Simulia are trademarks or registered trademarks of Dassault Systèmes or its subsidiaries in the United States and/or other countries.

applied for predicting other, independent results, and conclusions are drawn about the applicability of the PDA model. This study focuses on E-Glass Epoxy Laminates.

2 Progressive Damage Analysis (PDA)

The Abaqus PDA model is a generalization of the approach proposed by Camanho and Davila [15]. It requires linearly elastic behavior of the undamaged material and is used in combination with Hashin's damage initiation criteria [16].

2.1 Damage Initiation

In Abaqus [?] the onset of damage is detected by the Hashin and Rotem damage *initiation* criteria [16] in terms of apparent (nominal, Cauchy) stresses σ, which is calculated by the FEA code. Damage initiation refers to the onset of degradation at a material point. The criterion considers four different damage initiation mechanisms, which are assumed to be uncoupled, as follows

Fiber tension ($\sigma_{11} \geq 0$)

$$F_f^t = \left(\frac{\sigma_{11}}{F_{1t}}\right)^2 + \alpha\left(\frac{\sigma_{12}}{F_6}\right)^2 \tag{1}$$

Fiber compression ($\sigma_{11} < 0$)

$$F_f^c = \left(\frac{\sigma_{11}}{F_{1c}}\right)^2 \tag{2}$$

Matrix tension and/or shear ($\sigma_{22} \geq 0$)

$$F_m^t = \left(\frac{\sigma_{22}}{F_{2t}}\right)^2 + \left(\frac{\sigma_{12}}{F_6}\right)^2 \tag{3}$$

Matrix compression ($\sigma_{22} < 0$)

$$F_m^c = \left(\frac{\sigma_{22}}{2F_4}\right)^2 + \left[\left(\frac{F_{2c}}{2F_4}\right)^2 - 1\right]\frac{\sigma_{22}}{F_{2c}} + \left(\frac{\sigma_{12}}{F_6}\right)^2 \tag{4}$$

where σ_{ij} are the components of the stress tensor; F_{1t}, F_{1c}, are the tensile and compressive strengths in the fiber direction; F_{2t}, F_{2c}, are the tensile and compressive strengths in the matrix direction; F_6, F_4, are the longitudinal and transverse shear strengths, and α determines the contribution of the shear stress to the fiber tensile criterion. To obtain the model proposed by Hashin and Rotem [16] we set $\alpha = 0$ and $F_4 = 1/2\ F_{2C}$. Furthermore, $F_{ft}, F_{fc}, F_{mt}, F_{mc}$, are indexes that indicate whether a damage initiation criterion in a damage mode has been satisfied or not. Damage initiation occurs when any of the indexes exceeds 1.0.

The effect of damage is taken into account by reducing the values of stiffness coefficients [?, Section 21.3.1] as follows

$$\sigma = C : \varepsilon \tag{5}$$

where : represents a tensor double contraction and the damaged stiffness is given by

$$C = \begin{bmatrix} (1-d_f)E_1/\Delta & (1-d_f)(1-d_m)\nu_{21}E_1/\Delta & 0 \\ (1-d_f)(1-d_m)\nu_{12}E_2/\Delta & (1-d_m)E_2/\Delta & 0 \\ 0 & 0 & (1-d_s)G_{12} \end{bmatrix} \tag{6}$$

$$\Delta = 1 - (1-d_f)(1-d_m)\nu_{12}\nu_{21}$$

$$d_s = 1 - (1-d_f^t)(1-d_f^c)(1-d_m^t)(1-d_m^c) \tag{7}$$

where σ is the apparent stress, ε is the strain, C is the damaged stiffness matrix, E_1, E_2, are the moduli in the fiber direction and perpendicular to the fibers, respectively, G_{12} is the inplane shear modulus, ν_{12}, ν_{21}, are the inplane and Poisson's ratios, and $d_f^t, d_f^c, d_m^t, d_m^c, d_s$, are damage variables for fiber, matrix, and shear damage modes, in tension and compression, respectively. Note that the shear damage variable is not independent but given by (7) in terms of the remaining damage variables.

The damage variables $d_f^t, d_f^c, d_m^t, d_m^c$, that characterize fiber and matrix damage in tension and compression correspond to the four damage initiation modes (1–4). At any time, each material point is either in tension or compression. Therefore, the four damage variables reduce to two variables [**?**, Section 21.3.2] as follows

$$d_f = \begin{cases} d_f^t & \text{if} \quad \sigma_{11} \geq 0 \\ d_f^c & \text{if} \quad \sigma_{11} < 0 \end{cases} \tag{8}$$

and

$$d_m = \begin{cases} d_m^t & \text{if} \quad \sigma_{22} \geq 0 \\ d_m^c & \text{if} \quad \sigma_{22} < 0 \end{cases} \tag{9}$$

The six values of strength, $F_{1t}, F_{1c}, F_{2t}, F_{2c}, F_6, F_4$, are material properties that must be provided by the user. Due to differences between testing and application conditions, as well as in-situ effects [1, Section 7.2.1], the strength values measured by standard methods may not predict damage initiation accurately. Therefore, in this work, the values of strength are found by correlating model results to *laminate* experimental data.

The same equations (1–4) are used as damage *evolution* criteria by introducing effective stresses (10) in lieu of nominal stress. The relation between the effective stress $\widetilde{\sigma}$ and the apparent stress σ is computed [17, (8.64)] as

$$\widetilde{\sigma} = M^{-1} : \sigma \tag{10}$$

Abaqus PDA uses the model proposed by Matzenmiller et al. [18] to compute the degradation of the stiffness matrix coefficients. Therefore, the damage effect tensor in Voigt notation is given as

$$M^{-1} = \begin{bmatrix} (1-d_f)^{-1} & 0 & 0 \\ 0 & (1-d_m)^{-1} & 0 \\ 0 & 0 & (1-d_s)^{-1} \end{bmatrix} \tag{11}$$

Prior to damage initiation, the damage effect tensor M^{-1} is equal to the identity matrix, so $\widetilde{\sigma} = \sigma$. Once damage initiation and evolution has occurred for at least one mode, the damage effect tensor becomes significant in the criteria for damage initiation of other modes. When $d_f = 0$ and $d_m = d_s = 1$, equation (11) represents the degradation scheme of the ply discount method.

3 Damage Evolution

Once any of the damage initiation criteria (1–4) is satisfied, further loading will cause degradation of material stiffness coefficients. The evolution of the damage variable employs the critical energy release rates G_i^c, which are material properties, with *i=ft,fc,mt,mc,* corresponding to the four damage modes: fiber tension, fiber compression, matrix tension, and matrix compression, respectively. Therefore, in addition to six values of strength, four values of critical ERR must be provided, each one corresponding to the area of the triangle OAC shown in Fig. 1. This contrasts with other models where both onset and evolution of damage are predicted in terms of critical ERR only [19].

Normally, the constitutive model is expressed in terms of stress-strain equations. When the material exhibits strain-softening behavior, as shown in Fig. 1, such formulation results in strong mesh dependency. In Abaqus, to alleviate the mesh dependency in the PDA constitutive model, a characteristic length is introduced into the formulation. For membranes and shells the characteristic length L_c is computed as the square root of the area of the reference surface of the element. Using the characteristic length, the stress-strain constitutive model is transformed into the stress-displacement constitutive model illustrated in Fig. 1.

The evolution of each damage variable is governed by an equivalent displacement δ^{eq}. In this way, each damage mode is represented as a 1D stress-displacement problem (Fig. 1) even though the stress and strain fields of the actual problem are 3D. The equivalent displacement for each mode is expressed in terms of the components corresponding to the effective stress components used in the initiation criterion for each damage mode. The equivalent displacement and stress for each of the four damage modes are defined as follows [**?**, Section 21.3.3]

Fiber tension ($\sigma_{11} \geq 0$)

$$\begin{aligned} \delta_{eq}^{ft} &= L^C.\sqrt{\langle\varepsilon_{11}\rangle^2 + \alpha\varepsilon_{12}^2} \\ \sigma_{eq}^{ft} &= \frac{\langle\sigma_{11}\rangle\langle\varepsilon_{11}\rangle + \alpha\sigma_{12}\varepsilon_{12}}{\delta_{eq}^{ft}/L^c} \end{aligned} \tag{12}$$

Fiber compression ($\sigma_{11} < 0$)

$$\begin{aligned} \delta_{eq}^{fc} &= L^C\langle-\varepsilon_{11}\rangle \\ \sigma_{eq}^{fc} &= \frac{\langle-\sigma_{11}\rangle\langle-\varepsilon_{11}\rangle}{\delta_{eq}^{fc}/L^c} \end{aligned} \tag{13}$$

Matrix tension and shear ($\sigma_{22} \geq 0$)

$$\begin{aligned} \delta_{eq}^{mt} &= L^C\sqrt{\langle\varepsilon_{11}\rangle^2 + \varepsilon_{12}^2} \\ \sigma_{eq}^{mt} &= \frac{\langle\sigma_{22}\rangle\langle\varepsilon_{22}\rangle + \sigma_{12}\varepsilon_{12}}{\delta_{eq}^{mt}/L^c} \end{aligned} \tag{14}$$

Matrix compression ($\sigma_{22} < 0$)

$$\begin{aligned} \delta_{eq}^{mt} &= L^C\sqrt{\langle-\varepsilon_{22}\rangle^2 + \varepsilon_{12}^2} \\ \sigma_{eq}^{mt} &= \frac{\langle-\sigma_{22}\rangle\langle-\varepsilon_{22}\rangle + \sigma_{12}\varepsilon_{12}}{\delta_{eq}^{mc}/L^c} \end{aligned} \tag{15}$$

where $\langle\rangle$ represents the Macaulay operator, which is defined as $\langle\eta\rangle = \frac{1}{2}(\eta + |\eta|)$ for every $\eta \in \Re$.

For each mode, the damage variable controls the reduction of the stiffness coefficients, and may assume values between zero (undamaged state) and one (fully damage state). The damage variable for a particular mode is derived using Fig. 1 and given by given by

$$d = \frac{\delta_{eq}^C(\delta_{eq} - \delta_{eq}^0)}{\delta_{eq}(\delta_{eq}^C - \delta_{eq}^0)} \tag{16}$$

where δ_{eq}^C is the maximum value of δ_{eq} at point C in Fig. 1, for each mode.

Values of interlaminar critical energy release rates G^c reported in the literature are not directly applicable as input to Abaqus PDA because the damage addressed by PDA is intralaminar, not interlaminar. Also, the PDA model computes *equivalent* 1D energy release rates as the area under the curve on Fig. 1, not 3D energy release rates, which are defined as

$$G = -\frac{\partial U}{\partial A} \tag{17}$$

where the strain energy U is a 3D function of ε, and A is the crack area. Furthermore, in PDA, there is no identifiable crack but rather an equivalent reduction of stiffness. Therefore, the crack area A is not known and the ERR cannot be computed as in (17), but in terms of *equivalent* 1D stress and displacement (14).

4 Ply Discount

The ply discount method was used to compare to PDA results. The Hashin damage initiation criteria was implemented in a user subroutine based on (1–4), using nominal stress.

For damage evolution, the ply discount method simply reduces to zero the stiffness of the lamina that reaches the damage onset, except in the fiber direction which is left unchanged. In order to prevent convergence problems, the secant stiffness (6) is reduced using $d_f = 0, d_m = d_s = 0.999$, abruptly as soon as the Hashin damage initiation criteria (3) has been met.

Then, the stress is calculated with (5), where ε is total strain. In Abaqus, $\varepsilon_i = \varepsilon_{i-1} + \Delta\varepsilon_i$, where i is the current step. If damage has not initiated, the damage initiation criteria is evaluated for the recently calculated values of stress to decide whether or not the damage initiation criteria has been met. In ply discount, damage evolution is sudden and abrupt, occurring simultaneously with damage initiation.

5 Experimental

Changes in the normalized longitudinal Young's modulus and Poisson's ratio with respect to the applied strain, measured experimentally and reported in the literature, were used to compare with the Progressive Damage Analysis and the Ply Discount methodology. The laminate stacking sequences reported by Varna et al. in [20] and [21], shown in Table 1, were considered. The dimensions of the specimens are 20 mm wide with a free length of 110 mm. The ply properties for the laminates are listed in Table 2.

All laminates were subjected to axial deformation ε_x, which coincides with ε_{11} in the 0° laminas. None of the laminas in these laminates is subjected to fiber modes (1–2) or matrix compression (4). The 90° laminas in laminates #1 and #5 are subjected to pure traction and no shear, so damage initiation is controlled by the parameter F_{2t}. Therefore, the *laminate* experimental data for laminate #1 (Fig. 2(a)) was chosen to determine the insitu value of F_{2t}, which is reported in Table 3. This value is 100% higher than the UD strength reported in Table 2. When the insitu value is used to predict initiation for laminate #5, the predicted *first ply failure* (FPF) strain is 22.4% higher than the observed experimental data (Fig. 3(a)). The difference is due to insitu effect, because the damage initiation criteria used in Abaqus does not account for insitu effect.

6 Methodology

All the laminates considered for the study are symmetric and balanced. Therefore a quarter of the specimen was used for the analysis using symmetry b.c. and applying a uniform strain via imposed displacements on one end of the specimen. A longitudinal displacement of 1.1 mm was applied to reach a strain of 2%. Abaqus S8R elements were used for most of the study but the convergence study also considered S4R elements.

The value of apparent energy release rate G^c_{mt} was obtained simultaneously with the value of F_{2t} to provide a best fit with the PDA model to the experimental modulus data for the laminate #1 (Fig. 2(a)). Laminate #1 was chosen because only F_{2t} and G^c_{mt} are active. The experimental data and the fitted PDA model results are shown in Fig. 2(a).

Since numerical minimization algorithms only find local minima, it is important to first find a good guess for the adjustable parameters F_{2t} and G^c_{mt}. For this, 804 simulations were performed with random values of the parameters in the interval $1.5 < G^c_{mt} < 30.5\ kJ/m^2$ and $21 < F_{2t} < 141\ MPa$. The results are visualized in Figs. 4 and 5. The error was calculated using the usual formula

$$Error = \frac{1}{N}\sqrt{\sum_{i=1}^{N}\left(\left.\frac{E}{\widetilde{E}}\right|_{\varepsilon=\varepsilon_i}^{Abaqus} - \left.\frac{E}{\widetilde{E}}\right|_{\varepsilon=\varepsilon_i}^{exp}\right)^2} \tag{18}$$

where E and $\widetilde{E}$ now stand for the laminate longitudinal elastic modulus, damaged and intact respectively, and N is the number of experimental data points. Nineteen experimental data points are reported by Varna et al. [21].

Note that the shallow contour of error vs. G^c_{mt} in Fig. 4 may explain the great dispersion of values reported in the literature. In Fig. 4, a broad range of G^c_{mt} (10 to 30 kJ/m^2 in this case), seem to adjust more or less well the experimental degradation rate of modulus in Fig. 2(a). If the response measured (modulus) is weakly sensitive to the parameter of interest (G_{mt}^c), the experimental values of the parameter will have large scatter. Nevertheless, by adjusting simultaneously both parameters, F_{2t} and G_{mt}^c, the minimization algorithm described next is able to converge to a global minimum.

From Figs. 4 and 5, it can be seen that a good choice for initial guess is $G_{mt}^c = 12\ kJ/m^2$ and $F_{2t} = 80\ MPa$. Next, a MATLAB®script was executed to look for the minimum error (18), by repeatedly executing Abaqus with parameters varying as per the Simplex method [22]. The converged values of F_{2t} and G_{mt}^c are reported in Table 3.

According to (3), a combination of F_{2t} and F_6 determines the damage onset for off-axis plies. Since the values of F_{2t} and G_{mt}^c are already set, it only remains to adjust the insitu value of F_6, which is done by minimizing the error using the modulus data for laminate #8 because this is the laminate where the cracking laminas experience the most shear. Since Abaqus PDA uses the Hashin damage initiation criterion, equation (3) is active, F_{2t} is fixed and only F_6 can vary. A preliminary estimation of the error was obtained on 112 simulations by using random numbers in the range $27.5 < F_6 < 93\ MPa$. Varna et al. reported 13 experimental values [20, Fig. 13]. The error versus the longitudinal shear strength F_6 is presented in Fig. 6. From this plot, the initial guess value for the search was chosen to be $F_6 = 49\ MPa$. Once again, the MATLAB script was used to find the minimum error, at which point the converged value of F_6 is found and reported in Table 3.

7 Model Assessment

7.1 Comparison between PDA and Experimental Data

In this section we compare modulus and Poisson's ratio predicted with PDA vs. experimental data for the nine laminates listed in Table 1. Note that the modulus vs. strain data of laminate #1 was used previously to find values for F_{2t} and G_{mt}^c, and that only the damage initiation in laminate #8 was relevant in finding F_6. Since the remaining data has not been used to adjust the PDA parameters, it can be used for assessing the quality of the predictions.

The longitudinal modulus and Poisson's ratio for the nine laminates are compared with experimental data in Figs. 2 and 7–13. Figure 2(a) merely states the fact that F_{2t} and G_{mt}^c were adjusted using the data for this laminate. Figure 2(b) is a new result as it was not used to fit any parameters. It shows that the laminate Poisson's ratio is predicted well by the model.

As long as the cracking lamina is a 90° lamina (Figs. 3 and 7–9), PDA predictions are quite good, because both the insitu F_{2t} and G_{mt}^c are adjusted using a cracking 90° lamina. Even when the cracking lamina is at 70° with respect to the load direction, the cracks propagate predominantly under mode I, so the predictions of modulus is good (Fig. 10(a)).

However, cracking lamina under significant shear (Figs. 11–13) are not modeled well by PDA. This may be the result of the shear damage variable d_s not being an independent variable in the model. In fact, for the experimental data available, all the remaining modes of damage are absent. Substituting $d_f^t = d_f^c = d_m^c = 0$ in (7) yields $d_s = d_m^t$. That is, the reduction of shear modulus G_{12} represented by d_s is modeled as being equal to the reduction of transverse modulus E_2. This contrast with other models in the literature that use independent variables for d_s and d_m^t [23], etc. In fact, analytical computation of the reduction of stiffness after solving the equations of elasticity for a cracked laminate in [19, (23)] for laminate #8 yields a constant ratio $d_s/d_m^t = 0.69$ from crack initiation to saturation crack density. In contrast, the PDA ratio is $d_s/d_m^t = 1.0$.

Note that the data for laminate #8 was used to adjust F_6, an thus damage initiation is predicted accurately in Fig. 12(a), but G_{mt}^c was adjusted with laminate #1, and it cannot be readjusted with laminate #8, so the damage evolution is not predicted accurately.

7.2 Insitu Strength

Since the values of F_{2t} and F_6 reported in Table 3 were calculated to match *laminate* data, the values obtained are insitu values. To highlight the error incurred when using unidirectional (UD) lamina strength values rather than insitu values, a comparison is presented on Table 4 between the First Ply Failure (FPF) strain calculated with Abaqus and the FPF strain calculated using an online laminate analysis software (cadec-online.com) with and without insitu correction of the UD strength values. The UD strength values (without insitu correction) were back calculated using [1, (7.42)] in terms of the insitu values reported in Table 3 and assuming the transition thickness of the E-glass-epoxy material is 0.6 mm [24]. The Abaqus results are found to be in good agreement with the FPF values calculated using insitu strength into the Hashin damage initiation criterion implemented in the laminate analysis software [25]. However, as shown in column 4 of Table 4, the FPF strain is grossly underestimated if the insitu correction is neglected.

7.3 Convergence

In this section we assess the sensitivity of the Abaqus PDA model to h- and p-refinement, realized by mesh refinement and by changing the element type, respectively. Note that the specimen is subjected to a uniform state of membrane strain, so h-refinement should not be necessary to converge on a stress field, unless the constitutive model is mesh dependent.

However, the mesh convergence study reveals mesh dependency, as shown in Fig. 14. Before first ply failure (FPF), the force-displacement response is independent of the number of elements used in the mesh. After FPF, the force-displacement response diverge, revealing mesh dependency.

With n=140, asymptotic behavior at large strains is reached when the damage in the 90° lamina is fully developed. At this stage the laminate modulus reduces to one third of the undamaged value, as shown in Fig. 15. Also in Fig. 15, it can be seen that for an applied laminate strain $\varepsilon_x = 2.2\%$, the 0° lamina fails due to fiber tension, which is consistent with the fibers used in the laminates.

Modulus vs. strain for the $[0_2/90_4]_S$ laminate #1 are reported in Fig. 15. It can be seen that the model predictions are affected by the element type. Recall that the material parameters F_{2t}, F_6, G_{mt}^c, were adjusted using quadratic elements (S8R). Reduced integration (S8R5) yields identical results, but when the element is changed to linear (S4,S4R), the model predictions are significantly different, overestimating the modulus reduction.

8 Conclusions

A novel methodology is proposed to determine the material parameters, namely insitu strength F_{2t}, F_6, and critical ERR G_{mt}^c, using laminate experimental data. It is observed that PDA predictions are good for mode I matrix cracking but deficient for mixed mode matrix cracking including shear (laminates #7, #8, and #9). Also, the PDA model is not very sensitive to changes in the value of critical ERR, as shown by the shallow relationship of model error vs. critical ERR. This may explain the large dispersion of values reported in the litarature for the intra and interlaminar ERR. Compared to PDA, the ply discount method severely overestimates the stiffness changes and leads to large errors in the prediction of energy dissipation (toughness). However the asymptotic values of modulus reduction are reasonably accurate. Using PDA, all FPF predictions are reasonably good as long as the ply thickness of the cracked lamina are similar (4 plies in most of this study). However, a 20% insitu effect is shown when n=8 if the values of strength are not readjusted for insitu effect taking into account the change in thickness from 4 to 8 plies.

When the fiber tension, fiber compression, and matrix compression are not active, which is normally the case due to the high strength of the fibers and sudden brittle failure in compression, the PDA shear damage is equal to the PDA transverse tensile damage. Such constraint is likely responsible for the poor prediction shown when the cracking ply is subjected to shear. The present study used E-glass laminates to identify the PDA parameters because the reduction of laminate modulus due to transverse matrix damage in carbon fiber laminates is very small on account of the high modulus of the fibers. Therefore, it is unlikely that the proposed methodology would be applicable to carbon fiber laminates since the parameter identification relies on modulus vs. strain data. On the other hand, other models in the literature that are based on measurable state variables, such as crack density, can be identified using crack density, which is significant regardless of the fiber modulus.

Acknowledgements

This work was the result of a semester-long project in the 2012 course MAE 646 Advanced Mechanics of Composite Materials at West Virginia University, taught by the first author. The authors wish to express their gratitude to their classmates for their comments and collaboration during the semester with special mention and recognition to S. Koleti. Also, many thanks to Dr. A. Adumitroaie for introducing us to Abaqus PDA, as well as to Rene Sprunger and Simulia$^{\text{TM}}$ for their support of our educational programs.

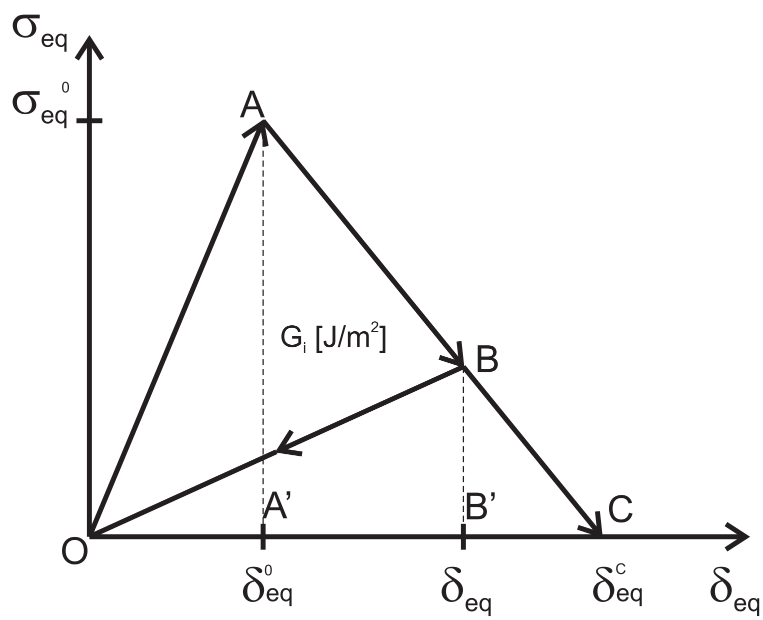

Figure 1: Equivalent stress versus equivalent displacement for a linearly softening material.

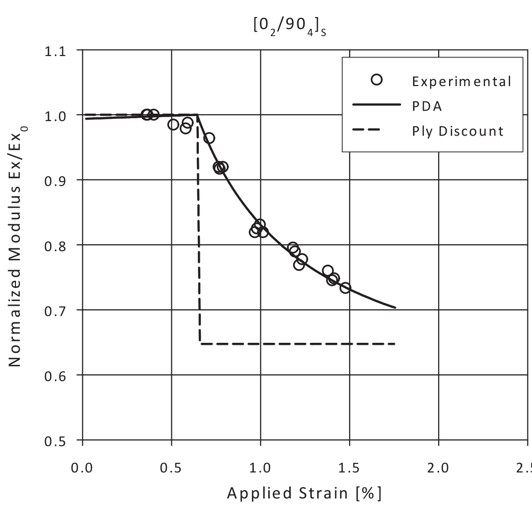

(a) Normalized modulus vs. applied strain.

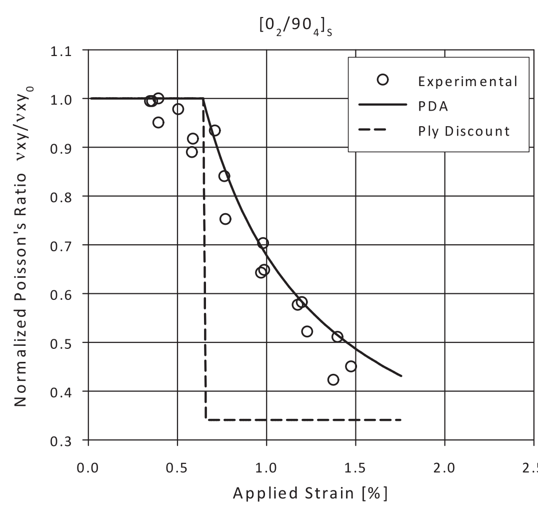

(b) Normalized Poisson's ratio vs. applied strain.

Figure 2: Laminate #1 with LSS $[0_2/90_4]_S$.

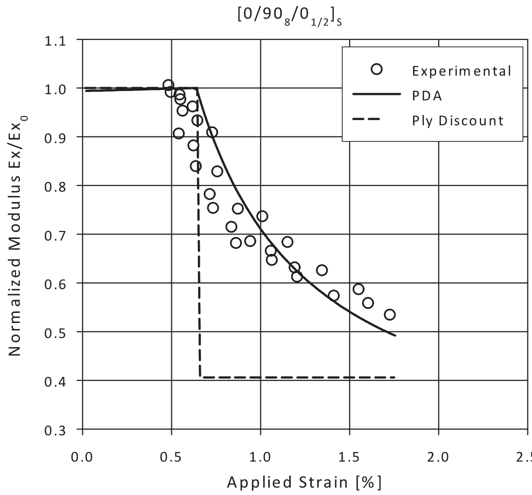

(a) Normalized modulus vs. applied strain.

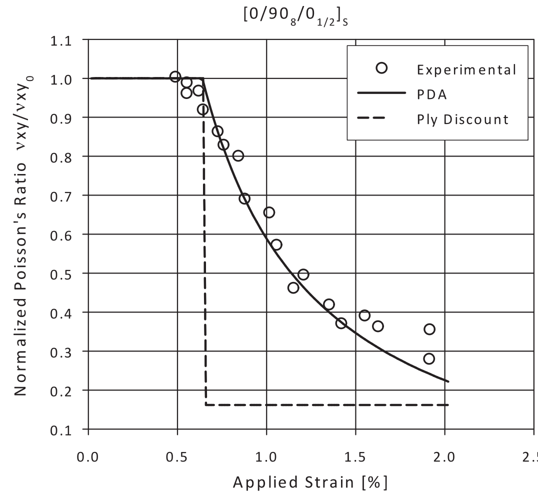

(b) Normalized Poisson's ratio vs. applied strain.

Figure 3: Laminate #5 with LSS $[0/90_8/0_{1/2}]_S$.

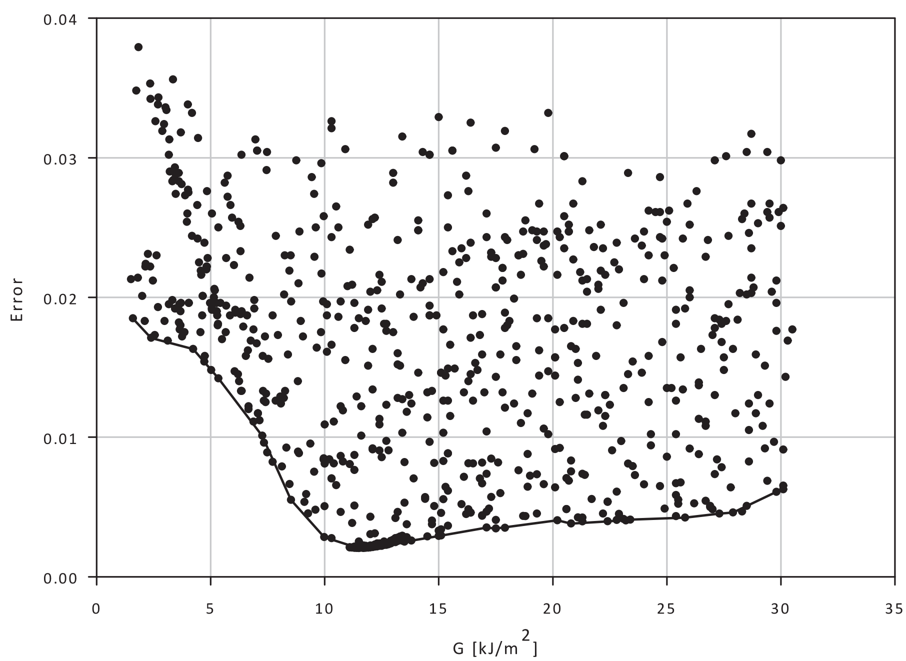

Figure 4: Error vs. G^c_{mt}.

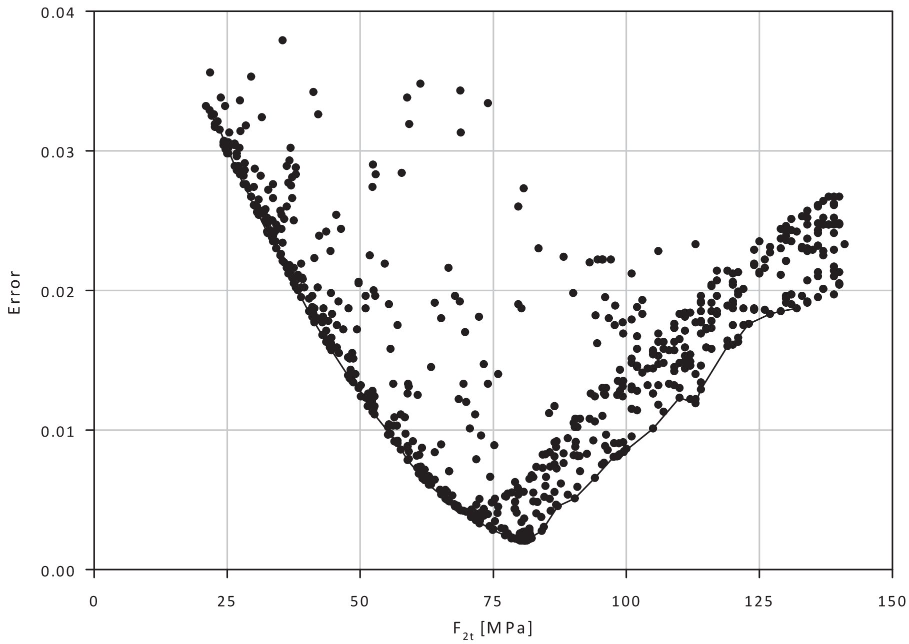

Figure 5: Error vs. F_{2t}.

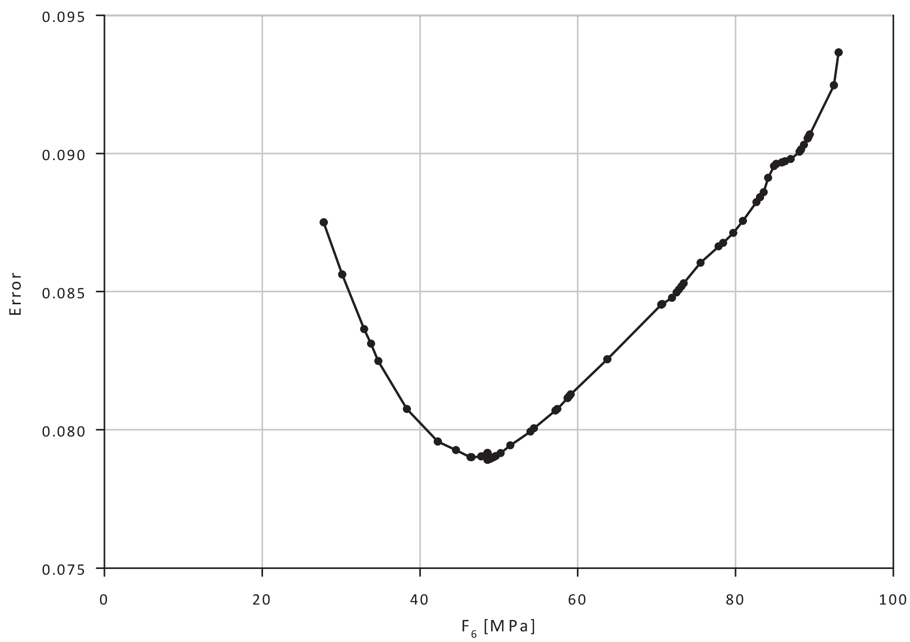

Figure 6: Error vs. F_6.

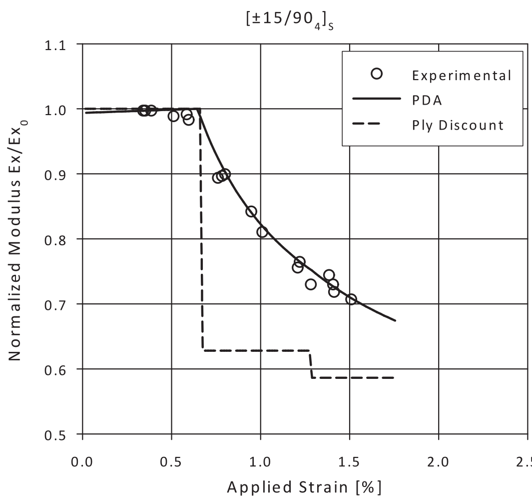

(a) Normalized modulus vs. applied strain.

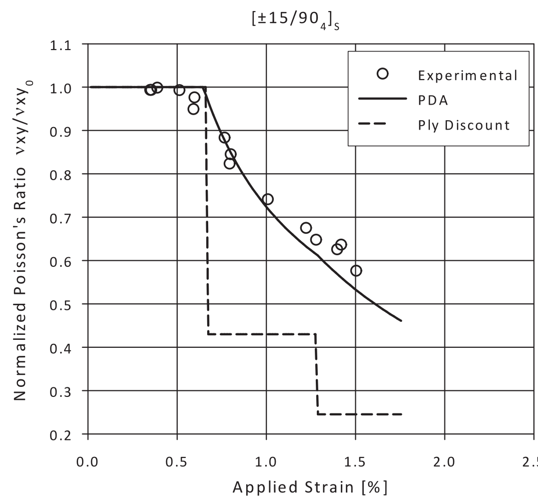

(b) Normalized Poisson's ratio vs. applied strain.

Figure 7: Laminate #2 with LSS $[\pm 15/90_4]_S$.

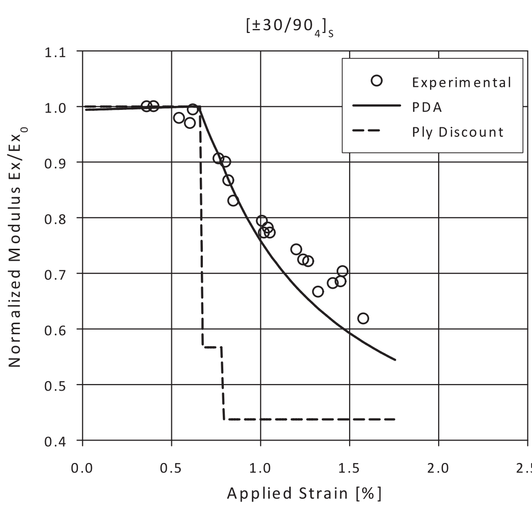

(a) Normalized modulus vs. applied strain.

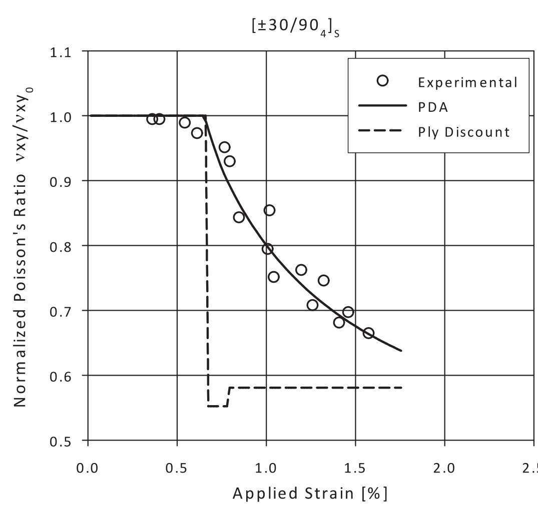

(b) Normalized Poisson's ratio vs. applied strain.

Figure 8: Laminate #3 with LSS $[\pm 30/90_4]_S$.

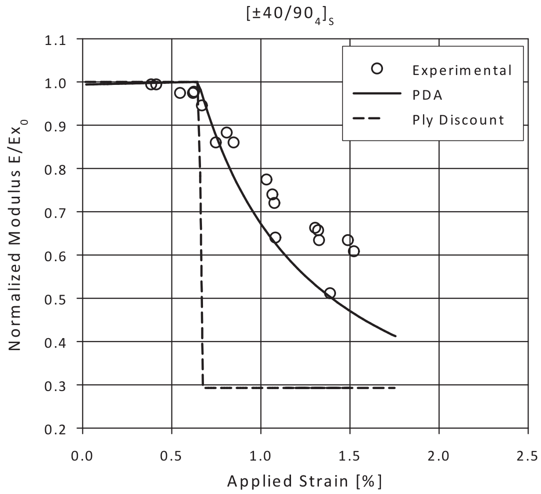

(a) Normalized modulus vs. applied strain.

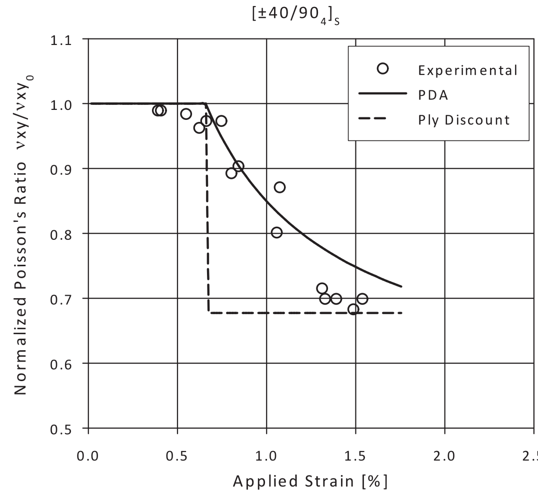

(b) Normalized Poisson's ratio vs. applied strain.

Figure 9: Laminate #4 with LSS $[\pm 40/90_4]_S$.

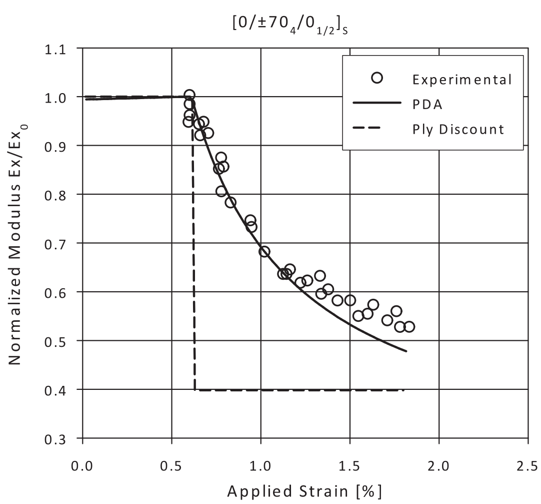

(a) Normalized modulus vs. applied strain.

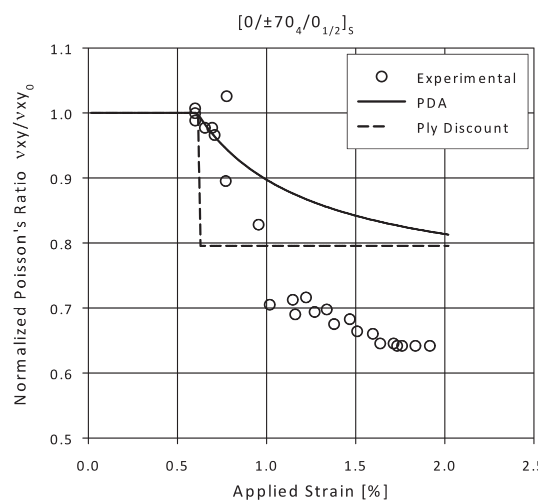

(b) Normalized Poisson's ratio vs. applied strain.

Figure 10: Laminate #6 with LSS $[0/\pm 70/0_{1/2}]_S$.

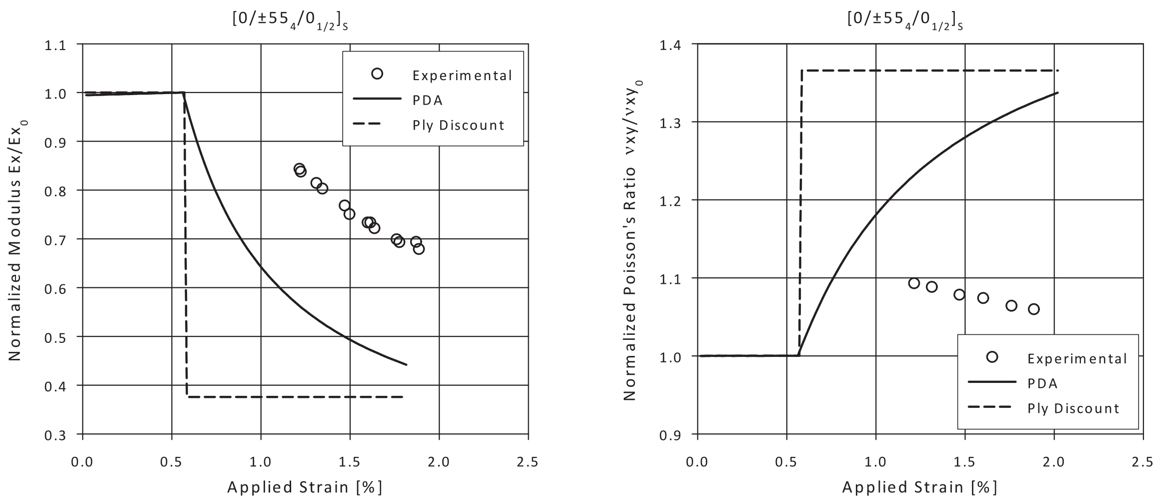

(a) Normalized modulus vs. applied strain. (b) Normalized Poisson's ratio vs. applied strain.

Figure 11: Laminate #7 with LSS $[0/\pm 55/0_{1/2}]_S$.

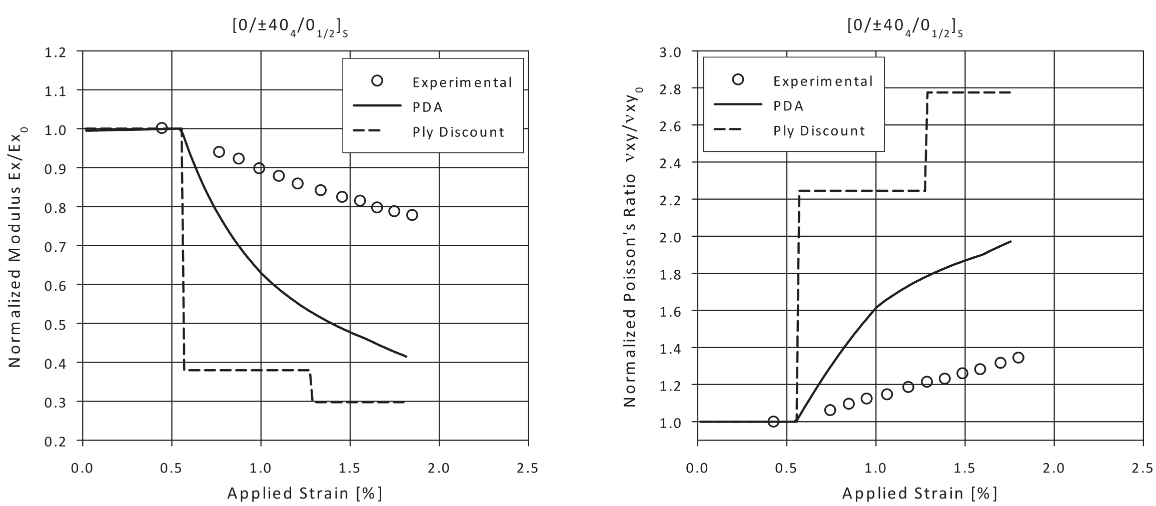

(a) Normalized modulus vs. applied strain. (b) Normalized Poisson's ratio vs. applied strain.

Figure 12: Laminate #8 with LSS $[0/\pm 40_4/0_{1/2}]_S$.

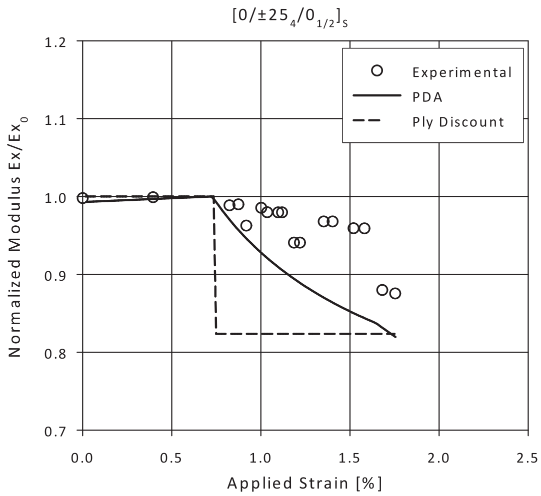

(a) Normalized modulus vs. applied strain.

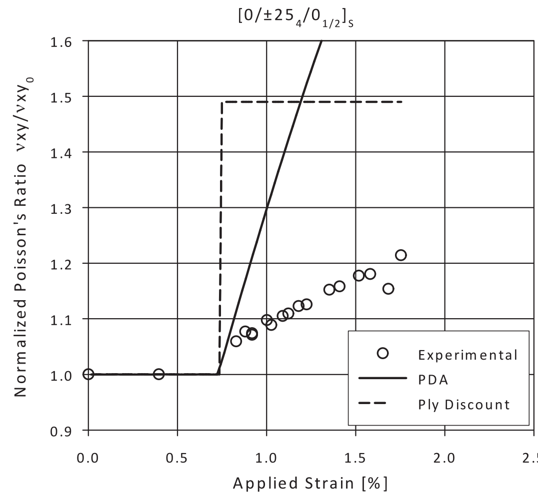

(b) Normalized Poisson's ratio vs. applied strain.

Figure 13: Laminate #9 with LSS $[0/\pm25/0_{1/2}]_S$.

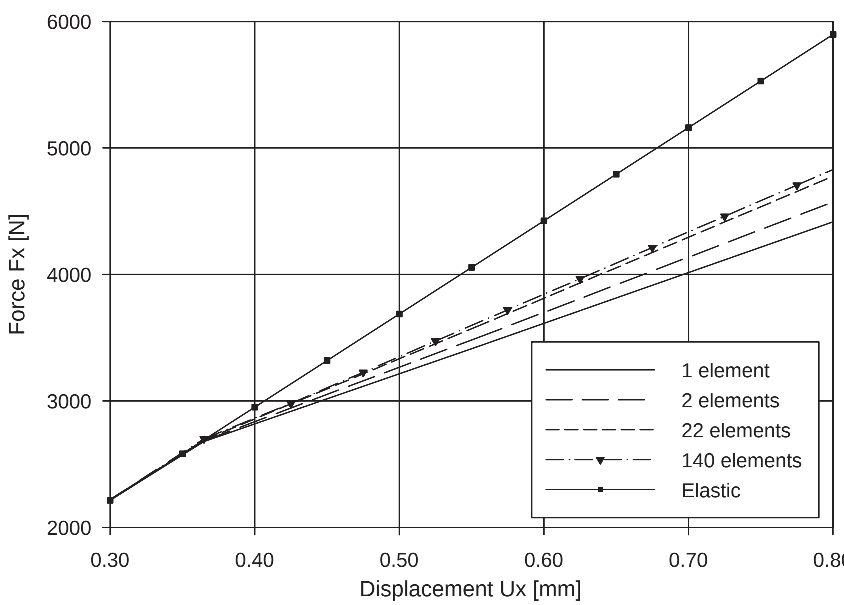

Figure 14: Force vs. displacement for laminate #8 using different elements. The elastic line goes through the origin (not shown).

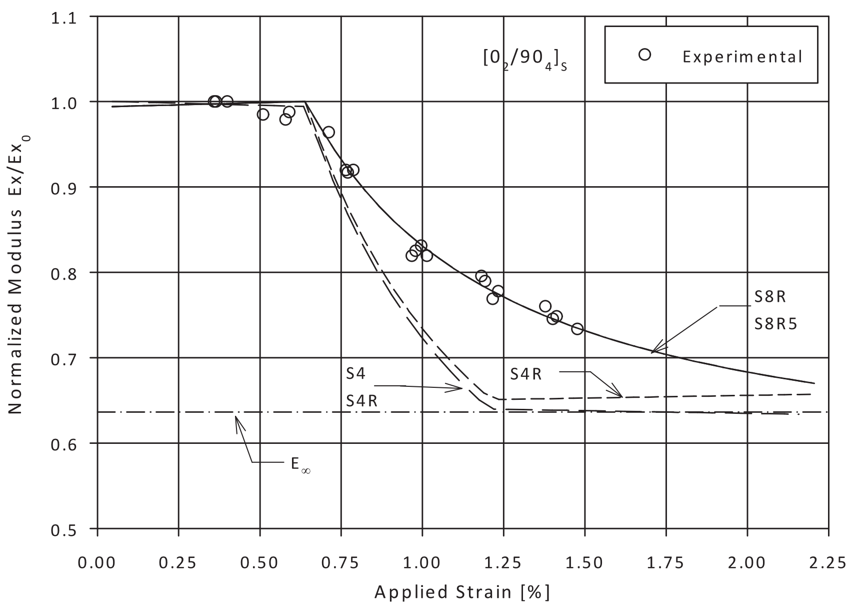

Figure 15: Normalized modulus vs. applied strain for laminate #8 using different types of elements ($\widetilde{E}_x = 68.22\ GPa$).

Table 1: Laminates considered in this study.

	LSS	Source
1	$[0_2/90_4]_S$	[21, Figs. 7]
2	$[\pm 15/90_4]_S$	[21, Figs. 8]
3	$[\pm 30/90_4]_S$	[21, Figs. 9]
4	$[\pm 40/90_4]_S$	[21, Figs. 10]
5	$[0/90_8/0_{1/2}]_S$	[20, Figs. 1,6,7]
6	$[0/\pm 70/0_{1/2}]_S$	[20, Figs. 2,9,10]
7	$[0/\pm 55/0_{1/2}]_S$	[20, Figs. 3,11,12]
8	$[0/\pm 40/0_{1/2}]_S$	[20, Figs. 13,14]
9	$[0/\pm 25/0_{1/2}]_S$	[20, Figs. 15,16]

Table 2: Unidirectional ply properties for glass/epoxy Fiberite HyE 9082Af. See Table 3 for insitu strengths.

Property	Units	Value	Source
E_1	[GPa]	44.7	[20]
E_2	[GPa]	12.7	[20]
G_{12}	[GPa]	5.8	[20]
G_{23}	[GPa]	4.5	[19]
ν_{12}	[GPa]	0.297	[20]
α_1	$[\mu\varepsilon/K]$	8.42	[26]
α_2	$[\mu\varepsilon/K]$	18.42	[20]
ΔT	[K]	-99	[20]
F_{1t}	[MPa]	1020	[17]
F_{2t}	[MPa]	40	[17]
F_{1c}	[MPa]	620	[17]
F_{2c}	[MPa]	140	[17]
F_6	[MPa]	60	[17]
ply thickness	[mm]	0.144	[21]

Tables

References

[1] E. J. Barbero. *Introduction to Composite Materials Design–Second Edition*. CRC Press, Boca Raton, FL, 2nd edition, 2010.

[2] R. J. Nuismer and S. C. Tan. Constitutive relations of a cracked composite lamina. *Journal of Composite Materials*, 22:306–321, 1988.

[3] S. C. Tan and R. J. Nuismer. A theory for progressive matrix cracking in composite laminates. *Journal of Composite Materials*, 23:1029–1047, 1989.

[4] S. Li, S. R. Reid, and P. D. Soden. A continuum damage model for transverse matrix cracking in laminated fibre-reinforced composites. *Philosophical Transactions of the Royal Society London, Series A (Mathematical, Physical and Engineering Sciences)*, 356:2379–2412, 1998.

Table 3: Insitu strengths and Apparent Energy Release Rate.

Property	Units	Value
F_{2t}	[MPa]	80.8831
F_6	[MPa]	48.5725
G_{mt}^c	$[\mathrm{kJ/m^2}]$	11.5002

Table 4: Comparison of FPF laminate strain ε_x using Abaqus with insitu values and cadec-online.com with and without insitu correction of strength.

	LSS	Abaqus with insitu	cadec-online.com with insitu	cadec-online.com without insitu
1	$[0_2/904]_S$	0.6420	0.6420	0.4053
2	$[\pm 15/90_4]_S$	0.6622	0.6452	0.4073
3	$[\pm 30/90_4]_S$	0.6622	0.6511	0.4111
4	$[\pm 40/90_4]_S$	0.6420	0.6387	0.4121
5	$[0/90_8/0_{1/2}]_S$	0.6420	0.6389	0.4034
6	$[0/\pm 70_4/0_{1/2}]_S$	0.6219	0.6094	0.3972
7	$[0/\pm 55_4/0_{1/2}]_S$	0.5817	0.5918	0.3837
8	$[0/\pm 40_4/0_{1/2}]_S$	0.5616	0.5514	0.3879
9	$[0/\pm 25_4/0_{1/2}]_S$	0.7427	0.7077	0.5069

[5] E. Adolfsson and P. Gudmundson. Matrix crack initiation and progression in composite laminates subjected to bending and extension. *International Journal of Solids and Structures*, 36:3131–3169, 1999.

[6] J. A. Nairn. *Polymer Matrix Composites*, volume 2 of *Comprehensive Composite Materials*, chapter Matrix Microcracking in Composites, pages 403–432. Elsevier Science, 2000.

[7] J. M Berthelot. Transverse cracking and delamination in cross-ply glass-fiber and carbon-fiber reinforced plastic laminates: static and fatigue loading. *Applied Mechanics Review*, 56:111–147, 2003.

[8] J. A. Nairn. *Finite Fracture Mechanics of Matrix Microcracking in Composites*, pages 207–212. Application of Fracture Mechanics to Polymers, Adhesives and Composites. Elsevier, 2004.

[9] S. H. Lim and S. Li. Energy release rates for transverse cracking and delaminations induced by transverse cracks in laminated composites. *Composites Part A*, 36(11):1467–1476, 2005.

[10] D. T. G. Katerelos, J. Varna, and C. Galiotis. Energy criterion for modeling damage evolution in cross-ply composite laminates. *Composites Science and Technology*, 68:2318–24, 2008.

[11] D. T. G. Katerelos, M. Kashtalyan, C. Soutis, and C. Galiotis. Matrix cracking in polymeric composites laminates: Modeling and experiments. *Composites Science and Technology*, 68:2310–17, 2008.

[12] J. A. Mayugo, P. P. Camanho, P. Maimi, and C. G. Dávila. Analytical modeling of transverse matrix cracking of $[\pm\theta/90_n]$ composite laminates under multiaxial loading. *Mechanics of Advanced Materials and Structures*, 17:237–45, 2010.

[13] GENOA Virtual Testing & Analysis Software, Alpha STAR Corporation, http://www.ascgenoa.com.

[14] Helius:MCT Composite Materials Analysis Software, Firehole Composites, http://www.firehole.com/products/mct/.

[15] P. Camanho and C. Davila. Mixed-mode decohesion finite elements for the simulation of delamination in composite materials. *NASA/TM-2002-211737*, pages 1–37, 2002.

[16] Z. Hashin and A. Rotem. A fatigue failure criterion for fiber-reinforced materials. *Journal of Composite Materials*, 7:448–464, 1973.

[17] E. J. Barbero. *Finite Element Analysis of Composite Materials*. Taylor & Francis, 2007.

[18] A. Matzenmiller, J. Lubliner, and R. Taylor. A constitutive model for anisotropic damage in fiber-composites. *Mechanics of Materials*, 20:125–152, 1995.

[19] E. Barbero and D. Cortes. A mechanistic model for transverse damage initiation, evolution, and stiffness reduction in laminated composites. *Composites Part B*, 41:124–132, 2010.

[20] J. Varna, R. Joffe, N. Akshantala, and R. Talreja. Damage in composite laminates with off-axis plies. *Composites Science and Technology*, 59:2139–2147, 1999.

[21] J. Varna, R. Joffe, and R. Talreja. A synergistic damage mechanics analysis of transverse cracking in $[\pm\theta/90_4]_s$ laminates. *Composites Science and Technology*, 61:657–665, 2001.

[22] J. Lagarias, J. Reeds, M. Wright, and P. Wright. Convergence properties of the nelder-mead simplex method in low dimensions. *SIAM Journal of Optimization*, 9:112–147, 1998.

[23] E. J. Barbero and L. De Vivo. Constitutive model for elastic damage in fiber-reinforced pmc laminae. *International Journal of Damage Mechanics*, 10(1):73–93, 2001.

[24] A. S. D. Wang. Fracture mechanics of sublaminate cracks in composite materials. *Compos. Tech. Review*, 6:45–62, 1984.

[25] Computer Aided Design Environment for Composites (CADEC) http://en.cadec-online.com.

[26] E. J. Barbero, G. Sgambitterra, A. Adumitroaie, and X. Martinez. A discrete constitutive model for transverse and shear damage of symmetric laminates with arbitrary stacking sequence. *Composite Structures*, 93:1021–1030, 2011.